Dual BRD4 and AURKA Inhibition Is Synergistic against MYCN-Amplified and Nonamplified Neuroblastoma[1]

Joshua Felgenhauer[*], Laura Tomino[*], Julia Selich-Anderson[*], Emily Bopp[†] and Nilay Shah[*‡]

[*]Nationwide Children's Hospital, Center for Childhood Cancer and Blood Disorders, 700 Children's Drive, Columbus, OH, 43205; [†]The Ohio State University, College of Arts and Sciences, 186 University Hall, Columbus, OH, 43210; [‡]The Ohio State University, College of Medicine, Department of Pediatrics, 370 W 9th Ave, Columbus, OH 43210

Abstract

A majority of cases of high-risk neuroblastoma, an embryonal childhood cancer, are driven by MYC or MYCN-driven oncogenic signaling. While considered to be directly "undruggable" therapeutically, MYC and MYCN can be repressed transcriptionally by inhibition of Bromodomain-containing protein 4 (BRD4) or destabilized post-translationally by inhibition of Aurora Kinase A (AURKA). Preclinical and early-phase clinical studies of BRD4 and AURKA inhibitors, however, show limited efficacy against neuroblastoma when used alone. We report our studies on the concomitant use of the BRD4 inhibitor I-BET151 and AURKA inhibitor alisertib. We show that, in vitro, the drugs act synergistically to inhibit viability in four models of high-risk neuroblastoma. We demonstrate that this synergy is driven, in part, by the ability of I-BET151 to mitigate reflexive upregulation of AURKA, MYC, and MYCN in response to AURKA inhibition. We then demonstrate that I-BET151 and alisertib are effective in prolonging survival in four xenograft neuroblastoma models in vivo, and this efficacy is augmented by the addition of the antitubule chemotherapeutic vincristine. These data suggest that epigenetic and posttranslational inhibition of MYC/MYCN-driven pathways may have significant clinical efficacy against neuroblastoma.

Neoplasia (2018) 20, 965–974

Introduction

Advanced neuroblastoma, the embryonal childhood cancer arising from sympathoadrenal precursors, remains a major clinical challenge. Patients with high-risk tumors at diagnosis are treated with aggressive multimodal chemotherapies, radiation therapy, and immunotherapy but suffer high rates of disease progression and/or recurrence, with cure rates ~50% [1,2]. Those patients with progressive neuroblastoma rarely have durable responses to current salvage therapies and die of disease [3]. MYCN and/or MYC amplification or overexpression have been shown to be oncogenic drivers in a majority of advanced neuroblastomas [4–7]. These proteins are transcription factors, promoting expression of numerous oncogenes and enhancing cell proliferation and survival [8], but also function as repressors of cell signaling [9,10] and as drivers of transcriptional elongation and activation of superenhancers through interactions with CDK7/9 and RNA polymerase II [11–13].

MYC and MYCN are difficult to therapeutically target directly, but novel agents have been designed to destabilize or repress these oncoproteins indirectly. One class of drugs against MYC/MYCN-driven cancers targets Aurora Kinase A (AURKA), a protein with multiple functions in cytokinesis [14] and in the stabilization of MYC and MYCN, by prevention of FBXW7-mediated ubiquitination [15].

The first-in-class drug, alisertib, showed efficacy against neuroblastoma, particularly MYCN-amplified disease, preclinically [16]. However, in the Phase 1 pediatric clinical trial, it had higher toxicity in children than in adults, limiting its maximally tolerated dose [17]. Alisertib failed to meet response criteria in multiple phase 2 studies when used alone [18–21] but is being examined in combination therapies.

A second class of drugs against MYC/MYCN-driven cancers inhibits the bromodomain and extraterminal motif (BET) chromatin-binding proteins. These proteins recognize and localize to acetylated lysine residues [22] and promote transcription by recruiting and phosphorylating components of RNA Polymerase II [23]. One BET protein, BRD4, has been shown to be active in cancers by promoting expression of multiple targets, including *CDK4/6* [24], *BCL2* [25], *MCL1* [26,27], *MYC* [28], and *MYCN* [29]. BRD4 inhibitors, developed for research and clinical use, have shown some preclinical efficacy against *MYCN*-amplified neuroblastoma but did not induce regression when used alone [25,29,30]. The cytostatic effects of BRD4 inhibitors suggest that these drugs may have limited effects clinically when used alone, particularly in diseases where BRD4 supports oncogenesis but is not the primary disease driver.

AURKA and BRD4 inhibitors both attack many common oncogenic drivers in distinct but complementary ways. In this study, we show that the AURKA inhibitor alisertib and the BRD4 inhibitor I-BET151 have significant synergy against neuroblastoma cell lines *in vitro*, inhibiting viability at significantly lower doses than when either drug is used alone. We show that cells treated with alisertib have a reflexive transcriptional upregulation of *AURKA*, *MYC*, and *MYCN*, but concomitant treatment with I-BET151 represses that upregulation. Treatment with both drugs is more effective at repressing expression of multiple oncoproteins, including MYC, MYCN, CDK4/6, AURKA, and BCL2. In four tumor xenograft models, I-BET151 and alisertib are more efficacious together in extending survival than either drug alone and induce tumor regression in an *MYCN*-amplified model. Furthermore, the addition of the anti-tubulin chemotherapeutic vincristine augments this effect, inducing durable tumor regression that is maintained after cessation of treatment in an *MYCN*-amplified model and an *MYCN*-nonamplified model and extending survival in a third *MYCN*-nonamplified model.

Materials and Methods

Cell Lines

SK-N-SH cell line was obtained from Javed Khan (National Cancer Institute, Bethesda, MD). SK-N-AS cell line was obtained from American Type Culture Collection (Manassas, VA). NB1643 and NB-SD cell lines were obtained from Peter Houghton (Greehey Children's Cancer Research Institute, San Antonio, TX). All cell lines were authenticated by PowerPlex16 short tandem repeat analysis (Promega) at the start of *in vitro* studies and again prior to *in vivo* studies. Cells were cultured in DMEM (Corning, Bedford, MA) with 10% FBS (PeakSerum, Wellington, CO) at 37°C with 5% CO_2 and confirmed to be free of *Mycoplasma* by SouthernBiotech Mycoplasma Detection Kit (Birmingham, AL), tested every 3 months.

Drugs

Alisertib was purchased from ApexBio (Houston, TX). I-BET151 was obtained from GlaxoSmithKline (Collegeville, PA). A list of primers and antibodies used can be found in the supplementary data.

Cell Viability Assay, Combination Index (CI) Analysis, and LIVE/DEAD Assay

NB-1643, SK-N-SH, NB-SD, and SK-N-AS cells were plated in 96-well plates at 25,000; 25,000; 25,000; and 5000 cells/well, respectively, in complete media in triplicate wells for each dose and cultured for 24 hours. Cells were treated with either I-BET151 dissolved in DMSO with concentration from 20 to 8000 nM, alisertib dissolved in ethanol with concentrations from 10 to 1000 nM, both drugs, or vehicle control for 48 hours. Cell viability was measured using the IncuCyte ZOOM live cell imaging system (Essen BioScience, Ann Arbor, MI) to track percent confluence of each well. Percentage confluence as compared to vehicle control was used to calculate treatment effect. IC50 and combination index (CI) values were calculated using Compusyn software (Combosyn, Inc., Paramus, NJ). The cells were also treated with the Invitrogen LIVE/DEAD viability/cytotoxicity assay (ThermoFisher Scientific, Waltham MA) using the manufacturer protocol. In brief, at the experiment end point, medium was removed from the cells and washed with PBS. The cells were then treated with PBS containing 1 μM calcein AM and 2 μM ethidium homodimer. Viable cells take up the calcein AM, and dead cells take up the ethidium homodimer. Cells were incubated for 45 minutes and then imaged using the IncuCyte Zoom with fluorescence imaging settings. Viability was assessed by green fluorescence; cytotoxicity was assessed by red fluorescence. Three independent experiments were performed; representative experiments are shown here.

Reverse Transcription–Quantitative Polymerase Chain Reaction (RT-qPCR)

Cells were grown to 80% confluence and then treated with 1 μM I-BET151, 1 μM alisertib, both drugs at 1 μM, or vehicle control for 24 hours. Total RNA was extracted from the cells using NucleoSpin RNA purification kit (Takara Bio USA), and 1 μg of RNA was used for cDNA synthesis using Maxima RT cDNA First Strand Synthesis kit (ThermoFisher Scientific). qPCR was performed using KiCqStart SYBR Green qPCR ReadyMix (Sigma-Aldrich, St. Louis, MO) using the ABI PRISM 7900HT thermal cycler (ThermoFisher Scientific), with relative quantitation by the ddC_t method as previously described [31]. Experiments were performed with technical duplicates on each plate and in three independent experiments, with the relative expression of each experiment used to calculate expression and standard deviation, plotted on each graph.

Western Blot

Cells were grown to 80% confluence and then treated with 1 μM I-BET151, 1 μM alisertib, both drugs at 1 μM, or vehicle control for 48 hours. Cells were collected by scraping and lysed using RIPA buffer, with 50 μg of protein/sample used for Western blot as previously described [31]. Blots were imaged by chemiluminescence using ECL Western Blotting Substrate (ThermoFisher Scientific). Band intensity was quantified using ImageQuant TL software (GE Healthcare, Marlborough, MA) and then normalized by comparing each band to its actin control sample then to the vehicle control sample to generate a ratio of relative expression. Experiments were performed in independent triplicate; representative images are shown here. Complete blots are shown in the Supplementary Data.

Tumor Xenograft Studies

A total of 5×10^6 cells of each type were suspended in PBS and mixed 1:1 in Matrigel (Corning) to a final volume of 100 μl and injected subcutaneously into the flanks of SCID mice (Envigo,

Indianapolis, IN), one injection per mouse. Tumors were grown to ~100-200 mm^3 as estimated by volume = (length × width^2)/2. Mice were then treated with the listed drug combinations, n = 5 per group, with drugs at the following doses and routes: I-BET151, injected intraperitoneally 20 mg/kg/day; alisertib, orally by gavage 20 mg/kg/ day; vincristine, injected intraperitoneally 0.1 mg/kg/dose once weekly (formulations in the Supplementary Data). Mice were treated 5 days × 5 weeks and then observed without treatment for 2 weeks. Mice were weighed and tumors measured twice weekly. Mice were euthanized at humane end points, when tumors attained 2000 mm^3, or at the end of the study, with tumors harvested. All studies were designed in accordance with Nationwide Children's Hospital Institutional Animal Care and Use Committee (IACUC) guidelines and performed under IACUC-approved protocols.

Statistical Analysis

All statistical analyses were completed using GraphPad Prism 7 (GraphPad Software, Inc., La Jolla, CA). Where appropriate, the two-tailed Student's t test was used to calculate significant differences between comparison groups in the experiments above. For multiple comparisons, one-way analysis of variance (ANOVA) was used with the Bonferroni correction for multiple comparisons against a single control. Mantel-Cox log-rank test was used for survival analyses.

Results

Synergy between I-BET151 and Alisertib Against Neuroblastoma Cells In Vitro

We first aimed to demonstrate if I-BET151 and alisertib had synergistic antineoplastic activity *in vitro*. We used SK-N-AS and SK-N-SH, *MYCN*-nonamplified cell lines, and NB-SD and NB1643, *MYCN*-amplified cell lines. We treated the cells with a range of doses of I-BET151 from 0 to 2000 nM and with alisertib from 0 to 1000 nM for 48 hours, defining IC50 doses for each drug and cell line (Supplementary Table 1). All cell lines were sensitive to both drugs, although alisertib was much more cytotoxic and I-BET151 was more cytostatic at 48 hours, as determined by viability and cytotoxicity staining with calcein AM and ethidium homodimer, respectively (Supplementary Figure 1). It was also noteworthy that NB-SD cells were less sensitive to alisertib than NB1643 cells, consistent with prior data [32]. We then treated the cells with all combinations of those doses and evaluated cell viability at 48 hours. Using Compusyn software, we found that, in all four cell lines, most drug combinations used were significantly synergistic in inhibiting cell proliferation and viability (Figure 1). The Compusyn software calculates, for each drug dose combination, the expected effects of the drugs alone and compares this to the observed effect, calculating a combination index (CI) [33]. CI < 1 shows a greater-than-additive effect of the drugs, and CI < 0.7 is considered synergistic. For all four cell lines, most drug dose combinations had CI < 0.7 and as low as 0.1. This supported our initial hypothesis that combined BRD4 and AURKA inhibition synergistically inhibits neuroblastoma viability.

Efficacy of I-BET151 and Alisertib in Repressing Target Protein Expression

We hypothesized that I-BET151 and alisertib exerted synergy due to complementary mechanisms of activity, namely, that I-BET151 would repress transcriptional expression of those proteins posttranslationally repressed by alisertib. We examined the transcriptional expression of a number of the gene targets of these drugs. SK-N-AS,
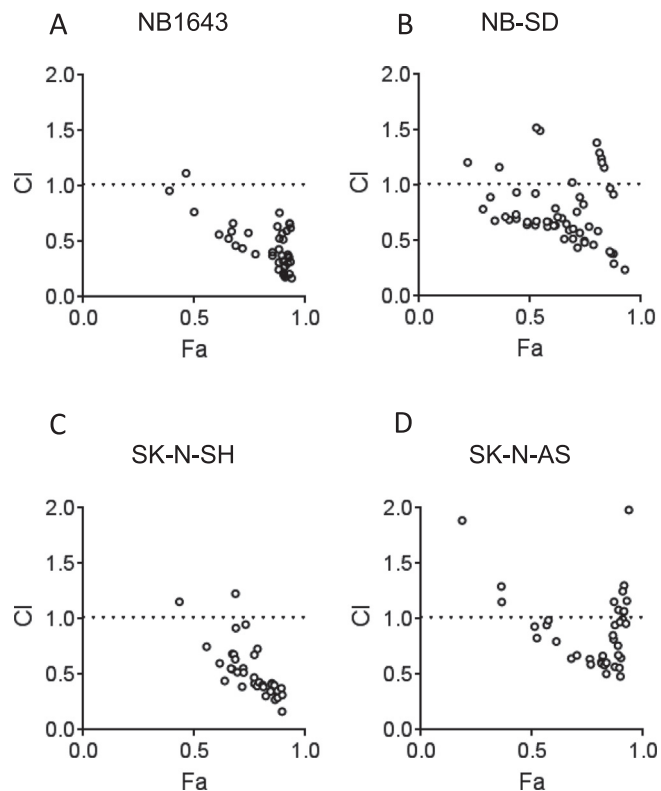

Figure 1. I-BET151 and alisertib are synergistic in their effects on neuroblastoma cell viability *in vitro*. Combination Index (CI) plots are shown for NB1643 (A), NB-SD (B), SK-N-SH (C), and SK-N-AS (D) neuroblastoma cell lines. Cells were treated with a combination of doses of I-BET151 and alisertib for 48 hours, as described in the methods, and images were obtained to quantify percentage confluence per well. Fraction affected (F_a) is defined as 100 − percent confluence and plotted on the x-axis. Each dose combination and the resultant F_a, as well as the F_a for each drug alone at individual doses, were entered into the Compusyn software. From these data, the CI for each dose combination was calculated, determined if the F_a observed was antagonistic (less than each drug's effect alone, CI >1), additive (equal to the effective of each drug alone, CI = 1), or greater-than additive (greater than the effect of each drug alone, CI <1). CI <0.7 is generally considered synergistic. For each cell line, a majority of drug combinations had CI <1, with F_a <0.5 for all such combinations. Representative experiments shown.

SK-N-SH, NB-SD, and NB1643 cells were treated with 1 μM of I-BET151, alisertib, both, or equal volume of vehicle for 24 hours and then harvested for RNA used for RT-qPCR. For most genes tested, we observed that treatment of the cells with I-BET151 repressed gene expression at 24 hours below levels seen in controls, whereas treatment with alisertib alone resulted in upregulation of those target genes, particularly *AURKA*, *MYC*, and *MYCN* (Figure 2). Use of I-BET151 with alisertib mitigated that upregulation, preventing compensation for AURKA inhibition (one-way ANOVA for SK-N-AS among the 4 treatment groups P = .0079, for SK-N-SH P = .0482, for NB-SD P = .0316, and for NB1643 P = .0169). The degree of these effects varied among the cell lines. In the *MYCN*-amplified NB1643 cells, I-BET151 had a modest effect on repression of gene expression alone, alisertib caused prominent "rebound" gene overexpression, but
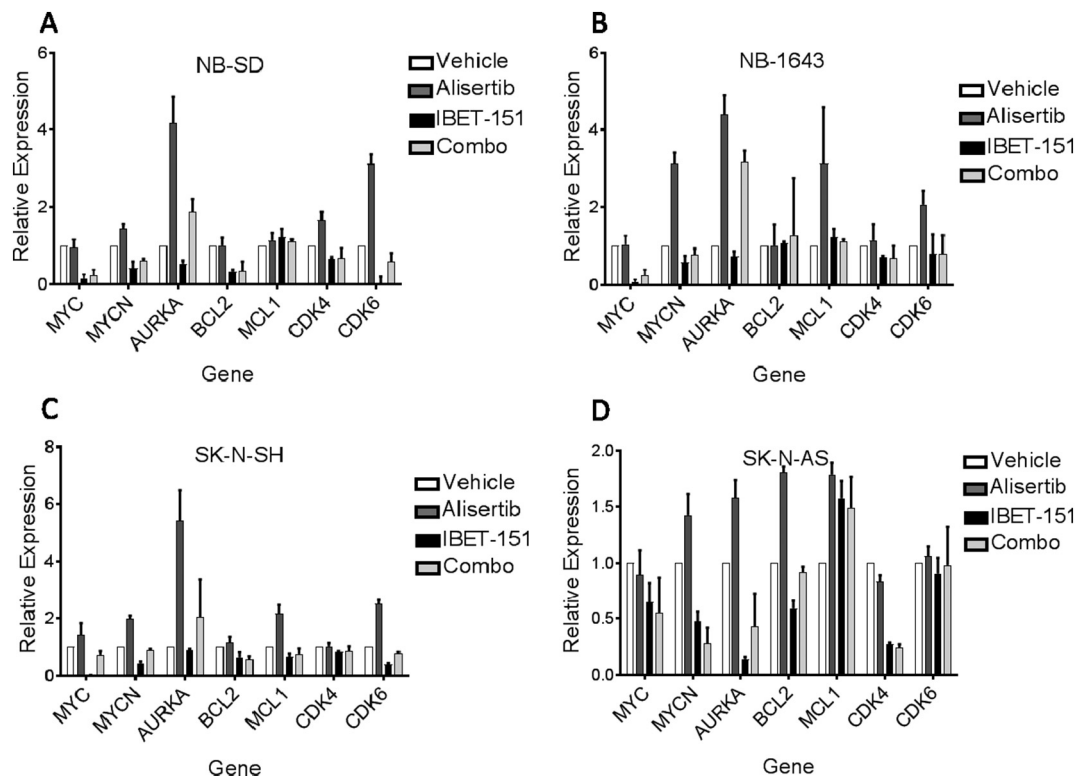
Figure 2. AURKA inhibition with alisertib induces increased RNA expression of oncogenes, which is mitigated by BRD4 inhibition with I-BET151. Cells were treated with 1 μM I-BET151, 1 μM alisertib, both drugs, or vehicle control for 24 hours, after which RNA was extracted from each cell line and used for RT-qPCR. Treatment with alisertib alone (dark gray bars) induced overexpression of most oncogenic targets tested in NB-SD (A), NB1643 (B) and SK-N-SH (C) cells, with less of an effect on SK-N-AS (D) cells except for *AURKA*. Co-treatment of the cells with I-BET151 reduced or entirely abrogated this overexpression for most target genes in all four cell lines. Relative expression shown using ddC$_t$ methods, with each gene's expression normalized first to housekeeping genes in each sample then against each gene's expression in the vehicle control. Three independent experiments performed, with mean and standard error plotted; one-way ANOVA based on treatment for NB-SD among the four treatment groups $P = 0316$, for NB1643 $P = .0169$, for SK-N-SH $P = .0482$, and for SK-N-AS $P = .0079$.

I-BET151 with alisertib had limited rebound gene expression for most genes tested, except for *AURKA* itself. The *MYCN*-amplified NB-SD cells and *MYCN*-nonamplified SK-N-SH cells had similar patterns of expression in response to the drugs, though with less rebound gene expression in response to alisertib and with more effective reduction of *AURKA* expression when both drugs were used. The *MYCN*-nonamplified SK-N-AS cells had the least amount of rebound gene expression in response to alisertib but had more consistent repression of gene expression by I-BET151, alone or with alisertib.

We confirmed the effects of this drug combination on protein expression by Western blot, including the effects on AURKA function, as evaluated by its capacity to autophosphorylate at threonine-288 ("p-AURKA"). In all four cell lines, we found that alisertib reduced levels of p-AURKA, demonstrating on-target effects that also correlated with decreased MYCN and MYC expression. I-BET151 alone was more effective at reduced total AURKA expression, however, and had correspondingly lower p-AURKA levels as compared to vehicle control, though not as low as alisertib. This decrease in AURKA expression also correlated with decreased MYCN and MYC expression. I-BET151 with alisertib was more effective than alisertib alone in repressing expression of multiple oncoproteins, including AURKA, MYC, MYCN, and CDK4/6 (Figure 3), mitigating reflexive protein overexpression in reaction to alisertib. More variable effects were seen on BCL2 and MCL1, with

MCL1 repressed in NB1643 and SK-N-SH cells, BCL2 repressed in NB-SD and SK-N-SH cells, but neither MCL1 nor BCL2 significantly affected by I-BET151 and/or alisertib in SK-N-AS cells. These data further supported our hypothesis that the two drugs can synergistically repress expression of common oncoprotein targets.

Synergy of I-BET151 and Alisertib against Neuroblastoma In Vivo

Given these preliminary data, we next evaluated the efficacy of these drugs *in vivo*. SK-N-SH, NB1643, NB-SD, and SK-N-AS cells were implanted subcutaneously into the flanks of SCID mice to generate tumor xenografts. When the xenografts were 100-200 mm^3 in volume, the mice were treated with I-BET151, alisertib, both drugs together, or vehicle alone to humane end point or for 5 weeks, with surviving mice observed for a drug washout period of 2 weeks. Each group of mice tolerated the treatments well, with no significant weight loss or indications of physiologic stress.

In the mice with SK-N-SH tumors, treatment with I-BET151 did not extend survival as compared to vehicle (Figure 4A, median survival 38 days vs 38 days, $P = .47$). Treatment with alisertib did extend survival (median survival 56 days, $P = .0064$), but only one mouse survived throughout the study. I-BET151 and alisertib together were superior to either drug alone (medial survival undefined, $P = .0018$ vs I-BET151, $P = .0416$ vs alisertib), with
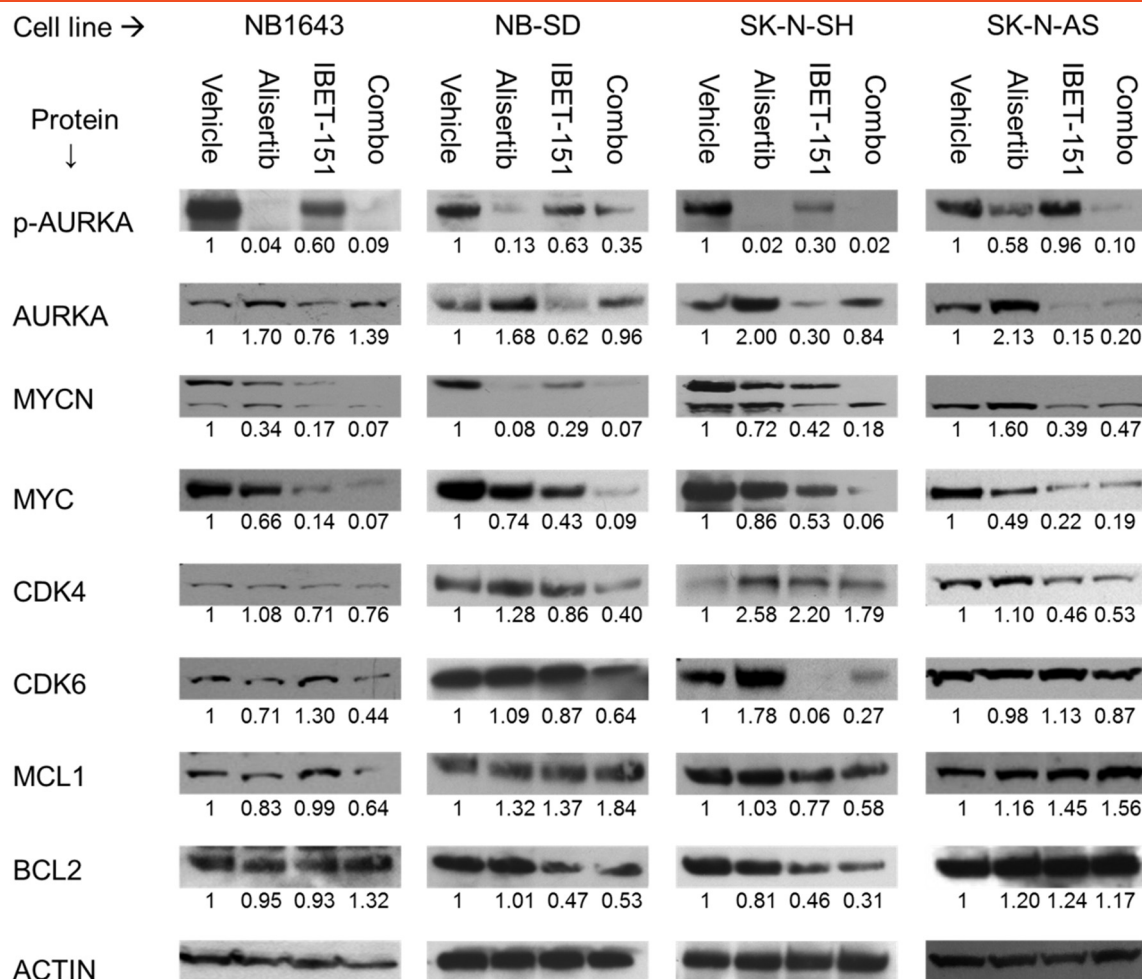
Figure 3. Dual AURKA and BRD4 inhibition is most efficacious in repressing target oncoprotein expression. Western blots of oncoprotein expression in four neuroblastoma cell lines. Cells were treated with 1 μM I-BET151, 1 μM alisertib, both drugs, or vehicle alone for 48 hours, after which cells were lysed and total protein harvested for Western blot. For all four cell lines, treatment with the AURKA inhibitor alisertib caused decreased p-AURKA levels and increased total AURKA expression, but with decreases in MYC and/or MYCN expression. Treatment with BRD4 inhibitor I-BET151 caused decreased in AURKA, MYC, and MYCN expression. Use of both inhibitors caused greater decrease in protein expression of AURKA, MYCN, and MYC as compared to alisertib alone in all three cell lines. Similar changes were seen on CDK4/6 and MCL1 in NB1643 and SK-N-SH cells and in CDK4 and BCL2 in NB-SD cells. SK-N-AS cells showed no effects on CDK6, MCL1, or BCL2 expression with any drug treatments. Immunoblot band intensity was quantified by densitometry and normalized against the actin control for each lane, then against the vehicle control for each cell line. Normalized expression for each band is shown directly below it. Three individual experiments were performed, with representative blots shown.

4/5 mice surviving through the washout period, though their tumors did regrow after treatment ended (Supplementary Figure 2A).

In the mice with NB1643 tumors, treatment with I-BET151 trended toward significantly extending survival as compared to vehicle alone (Figure 4B, median survival 57 days vs 41 days, $P = .069$). Treatment with alisertib strongly significantly extended survival as compared to vehicle (median survival undefined, $P = .0090$), with 4/5 mice surviving through therapy and washout. Treatment with I-BET151 and alisertib similarly extended survival as compared to vehicle (median survival undefined, $P = .0018$). However, tumor growth was different between those mice treated with alisertib alone as compared to with both drugs (Supplementary Figure 2, D and E). Of the mice treated with alisertib alone, 3/4 mice had their tumors regrow after the end of treatment. In contrast, only 1/4 mice treated with both drugs had its tumor grow appreciably after treatment ended, suggesting that the drug combination had a more durable

antitumor effect against this *MYCN*-amplified tumor xenograft model.

In the mice with NB-SD tumors, treatment with I-BET151 did significantly extend survival as compared to vehicle alone (Figure 4C, median survival 46 days vs 40 days, $P = .0485$). Treatment with alisertib alone also significantly extended survival as compared to vehicle alone (median survival 50 days, $P = .0203$) and trended toward improved survival as compared to I-BET151 ($P = .1254$), but no mice survived the treatment and washout periods. Treatment with I-BET151 and alisertib was significantly more effective at extending survival compared to either drug alone (median survival undefined, $P = .0018$ vs I-BET151, $P = .0255$ vs alisertib), with 3/5 mice surviving therapy and washout. Of these mice, one mouse had only modest growth of its tumor during the washout period, and the other two had effectively stable disease burden (Supplementary Figure 2F). This again suggests that the drug combination of I-BET151 and
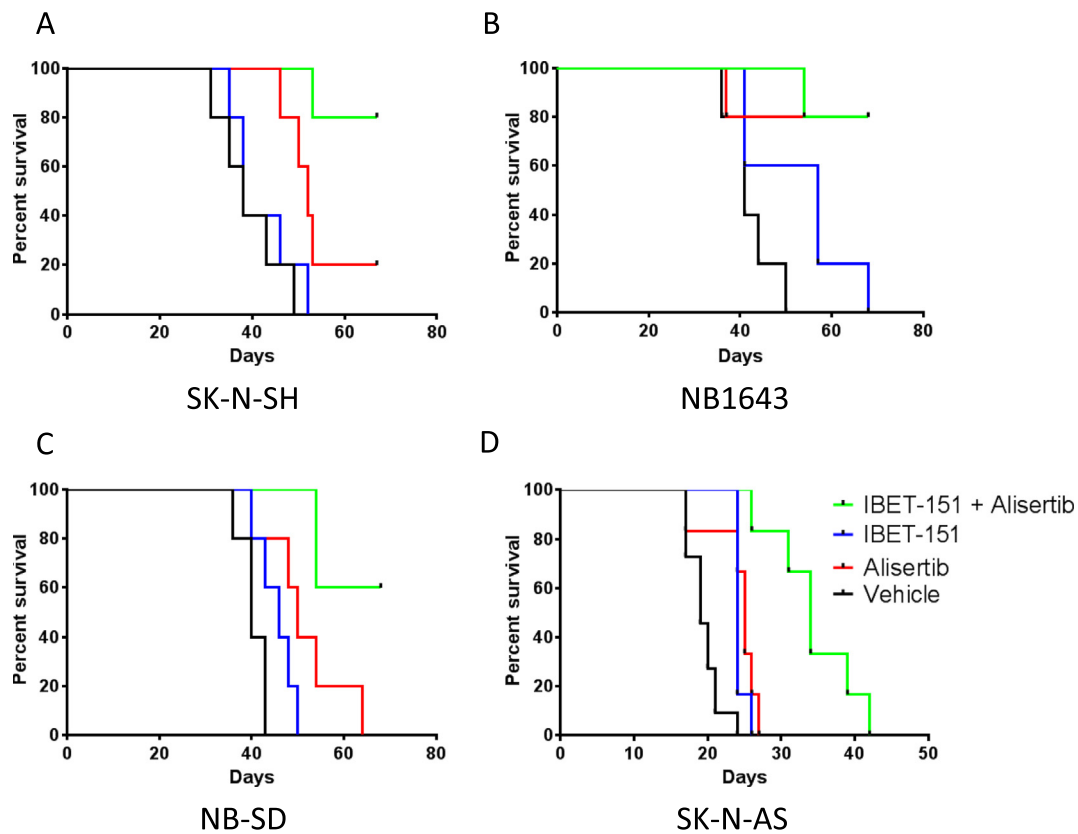
Figure 4. Drug combinations of I-BET151 and alisertib improve survival of mice with neuroblastoma tumor xenografts. Kaplan-Meier survival curves of tumor xenograft studies. See main text for description of treatment methods; $n = 5$ mice per treatment group. For mice treated with I-BET151, alisertib, both drugs, or vehicle alone, the two-drug combination was most efficacious as compared to vehicle control in extending survival (see main text for individual comparisons and P values, calculated by Mantel-Cox log-rank test).

alisertib has a durable antitumor effect against this *MYCN*-amplified neuroblastoma model.

In the mice with SK-N-AS tumors, treatment with either I-BET151 or alisertib significantly extended survival as compared to mice treated with vehicle (Figure 4C, median survival 24 vs 19 days, $P = .0009$, for I-BET151 vs vehicle, and median survival 25 vs 19 days, $P = .0038$, for alisertib vs vehicle). Treatment with both drugs together was superior to treatment with either drug alone (median survival 34 days, $P < .005$ as compared with vehicle or either drug alone), though the combination did not halt tumor growth fully in any of these mice. Nonetheless, these data were supportive of improved efficacy of BRD4 and AURKA inhibition in combination against all subtypes of neuroblastoma.

Synergy and Durable Response of Vincristine with I-BET151 and Alisertib Against Neuroblastoma In Vivo

The results of the tumor xenograft studies suggested that, while the combination of I-BET151 and alisertib was tolerated by the mice and improved overall survival, there was either a delayed or incomplete antitumor effect of the drug combination against neuroblastoma *in vivo*. We hypothesized that addition of a cytotoxic chemotherapeutic could improve the efficacy of the drug combination. Vincristine, a vinca alkaloid that inhibits tubulin polymerization, has been shown to be synergistic in other cancers with both BRD4 inhibitors [34] and AURKA inhibitors [35]. For this and additional reasons discussed

below, we evaluated the efficacy of vincristine with I-BET151, with alisertib, and in combination with both drugs.

A pilot study identified that, while mice tolerated vincristine dosing of 0.2 mg/kg intraperitoneally weekly alone or with alisertib, they did not tolerate that dose in combination with I-BET151, with increased vincristine toxicity, urinary retention, and weight loss. Accordingly, we reduced the vincristine dosage to 0.1 mg/kg weekly. Given the high sensitivity of NB-1643 xenografts to alisertib alone and with I-BET151, we did not expect to be able to identify meaningful improvements in survival with the addition of vincristine. We instead used xenografts from the three other neuroblastoma cell lines.

Mice harboring SK-N-SH xenografts had a modest benefit from treatment with vincristine alone vs vehicle control (median survival 48 days vs 38, $P = .08$, Figure 5A). Vincristine with I-BET151 did significantly extend survival vs vehicle (median survival 53 days, $P = .0018$) but not more than vincristine alone ($P = .33$). Vincristine with alisertib extended survival as compared to vincristine alone or with I-BET151 (median survival 67 days, $P = .0018$ vs vehicle or vincristine, $P = .015$ vs vincristine+I-BET151), though not significantly better than I-BET151 with alisertib ($P = .32$). Vincristine with alisertib did maintain survival throughout the treatment period for all mice, but all tumors regrew during the washout period (Supplementary Figure 2B). Treatment with all three drugs was highly efficacious at extending survival as compared to vincristine with or without I-BET151 (median survival undefined, P = .0018 vs vincristine or
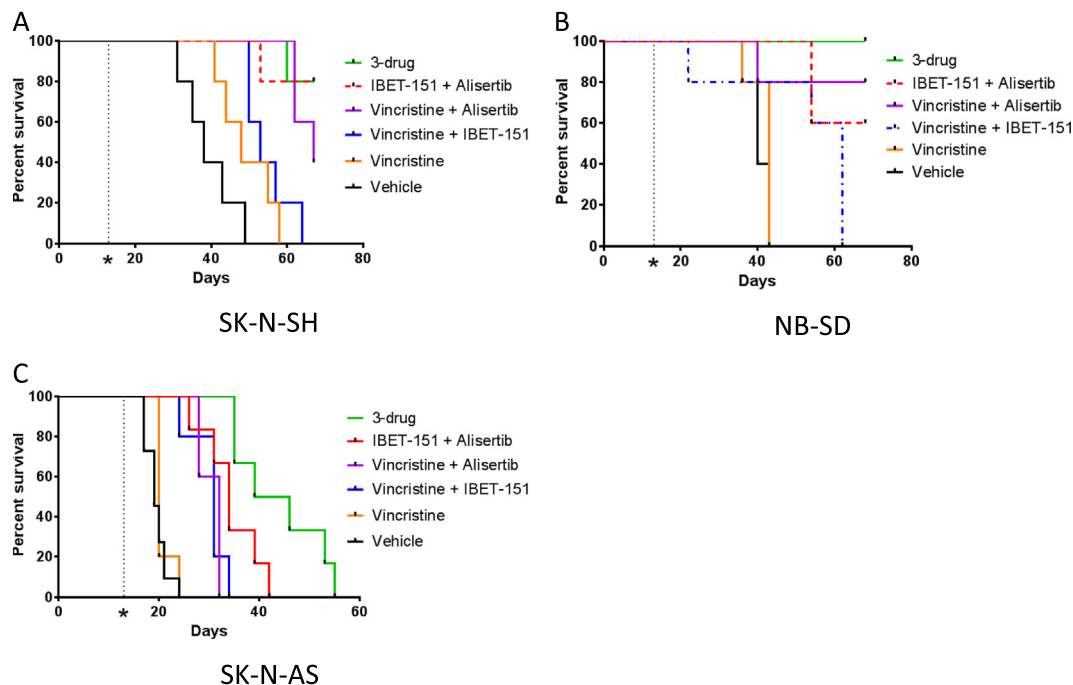
Figure 5. Drug combinations of I-BET151 and alisertib with vincristine improve survival of mice with neuroblastoma tumor xenografts. Kaplan-Meier survival curves of tumor xenograft studies. See main text for description of treatment methods; $n = 5$ mice per treatment group. For mice treated with various combinations of I-BET151, alisertib, vincristine, and vehicle, the three-drug combination was most efficacious as compared to vehicle in extending survival (see main text for individual comparisons and P values, calculated by Mantel-Cox log-rank test).

control, $P = .0062$ vs vincristine +I-BET151), though not significantly better than alisertib with I-BET151 ($P = .9372$) or with vincristine (P = .32). However, in striking contrast to all other treatment, use of vincristine, alisertib, and I-BET151 maintained repression of tumor growth through the washout period for 4/5 mice, inducing durable complete regressions (Supplementary Figure 2C).

Mice harboring NB-SD xenografts responded similarly to the drug combinations. Vincristine did not significantly improve survival compared to vehicle (median survival 43 vs 40 days, $P = .2845$, Figure 5B). Vincristine with I-BET151 improved survival vs vehicle (median survival 62 days, $P = .044$) and trended toward significant improvement vs vincristine alone ($P = .059$). Vincristine with alisertib significantly improved survival compared to these treatments (median survival undefined, $P = .02$ vs vehicle, $P = .046$ vs vincristine, and $P = .041$ vs vincristine and I-BET151). Four of the five mice treated with vincristine and alisertib survived the entire study, but all mice had tumor growth during the washout period (Supplementary Figure 2G). The three drugs together further improved survival (median survival undefined, $P = .0026$ vs vehicle, $P = .0035$ vs vincristine, $P = .0034$ vs vincristine and I-BET151, $P = .32$ vs vincristine and alisertib). More importantly, all 5 mice survived the entire study, 4 of 5 mice had no significant regrowth during the washout period, and only one tumor had growth during the washout period but still remained <500 mm³ (Supplementary Figure 2H).

Mice harboring SK-N-AS xenografts also benefited from the addition of vincristine, though to a less pronounced degree. Vincristine did not improve survival compared to vehicle (median survival 20 vs 19 days, $P = .27$, Figure 5C). Vincristine with I-BET151 was significantly more efficacious than vehicle or vincristine (median survival 31 days, $P = .0008$ vs vehicle, $P =$

.0047 vs vincristine). Vincristine with alisertib improved survival (median survival 32 days) as compared to vehicle ($P = .0004$) or vincristine ($P = .0016$) but not as compared to vincristine and I-BET151 ($P = .90$), in contrast to the other xenograft models. The three-drug combination was most effective at extending survival (median survival 46 days, P = .0004 vs control, 0.0016 vs vincristine, $P = .0020$ vs vincristine and I-BET151, $P = .0031$ vs vincristine and alisertib, $P = .027$ vs I-BET151 and alisertib). However, while the three-drug combination slowed tumor growth, none of the mice survived through the treatment course. Nonetheless, these data support efficacy of chemotherapy with BRD4 and AURKA inhibition against multiple types of neuroblastoma.

Discussion

MYCN or *MYC* amplification and/or overexpression have been shown to be the oncogenic drivers in over half of high-risk neuroblastomas [4,36–38]. These transcription factors have been generally considered to be "undruggable" therapeutic targets directly, but studies into the regulation and stabilization of MYC/MYCN identified indirect approaches to impair their tumorigenic programs. Repression of transcriptional expression by BRD4 inhibition and posttranslational destabilization by AURKA inhibition both demonstrated efficacy *in vitro* against neuroblastoma. However, these approaches in isolation failed to have significant efficacy in clinical trials. Our data show that combined BRD4 and AURKA inhibition is synergistic in against MYC/MYCN-associated oncogenic pathways. In particular, we demonstrated that BRD4 inhibition by I-BET151 induces transcriptional repression of defined BRD4 targets, as demonstrated by prior work in neuroblastoma specifically [29,30]. We also demonstrated inhibition of AURKA kinase function by

alisertib, as confirmed by repression of its autophosphorylation and concomitant MYC/MYCN repression, also consistent with prior work [39]. While this does not preclude other biological impacts of the drugs on neuroblastoma biology, it does confirm the on-target effects of each drug alone and together. This combination has efficacy against MYCN-amplified and nonamplified models of neuroblastoma *in vivo*, and this efficacy is further augmented by use of chemotherapy such as vincristine.

The comparative efficacy of BRD4 and AURKA inhibition varied in our neuroblastoma models with some association with their genomic alterations. NB1643 and NB-SD cell lines harbor *MYC-N*-amplification, while SK-N-SH and SK-N-AS cell lines do not. Additionally, SK-N-AS cells have unbalanced loss of heterozygosity (LOH) of chromosome 11q, a demonstrated clinical biomarker of poor prognosis [40,41]. In the combinatorial *in vitro* assay, the drugs were synergistic in all four models tested but with different dose effects. In the synergy plot (Figure 1), the x-axis indicates the F_a value, the percentage of cells affected at the experimental endpoint. In our experiment, this was defined as 100–% confluence to define the reduction of viable cells. The NB1643 cells had very high sensitivity to the synergistic effects of drugs, with F_a >0.8 and CI <0.7 for a majority of drug dosage combinations tested. We ascribed this to the sensitivity to alisertib, as reduction of the alisertib dose to 10 nM reduced the F_a of combinations to <0.7. The other cell lines were comparatively less sensitive to alisertib alone but still showed significant synergy, with CI <0.7 across the range of F_a.

This mirrored drug efficacy in the tumor xenograft models, in which the *MYCN*-amplified NB1643 and NB-SD xenografts had significantly higher sensitivity to alisertib-including combinations as compared to SK-N-SH and SK-N-AS. We theorize that this is due to the addiction of *MYCN*-amplified neuroblastoma to the MYCN--driven oncogenic pathways, making them very sensitive to any destabilization of MYCN. There was benefit in all models with the addition of I-BET151 but greater benefit in the MYCN-nonamplified SK-N-SH and SK-NAS xenografts. This could be because the SK-N-SH and SK-N-AS cells are less addicted to MYC/MYCN biology and more dependent on other oncogenic pathways affected by BRD4 inhibition, including cell cycle progression, cytokinesis, and antiapoptosis, as shown in the expression analyses (Figures 2 and 3).

While the drug combination did improve survival in mice with SK-N-AS xenografts, I-BET151 and alisertib were not as efficacious in inducing tumor regression as in the other models. The expression analyses showed that there was less effect of either drug alone or together on some pathways, particularly on MCL1 expression (Figures 2D and 3). It is possible SK-N-AS cells may survive by activation of antiapoptotic pathways by MCL1, which may or may not be due to LOH of 11q. SK-N-AS has also been shown to be chemotherapy-resistant [42,43] and has particularly high expression of ABCC1, which allows for drug efflux [44]. Thus, resistance to I-BET151 and alisertib may be due to elimination of the drugs before there is sufficient exposure for durable effect. Evaluation of the resistance mechanisms against BRD4 and AURKA inhibition is warranted in other models of neuroblastoma with LOH of 11q or ABCC1 expression.

Although alisertib showed preclinical antitumor efficacy, it failed to show meaningful activity in single-agent use in multiple clinical trials [18,21,45], in which it was administered for 7 days with 14 days of recovery. We have shown that alisertib treatment induces rebound transcriptional and protein overexpression of its targets, which may be

a mechanism of resistance against the drug and account for the lack of clinical efficacy. This rebound expression can be repressed by BRD4 inhibition, which we hypothesize allows for greater antitumor efficacy. This finding may impact future clinical trial design, whereby direct enzymatic inhibition, such as with alisertib, delivered in a pulsatile fashion may be best matched with chronic use of an epigenetic inhibitor, such as I-BET151, to prevent oncogenic reactivation and maintain tumor regression.

It is important to note that while AURKA protein expression was lower in cells treated with I-BET151 and alisertib together as compared to alisertib alone, it was not as low as I-BET151 alone. This emphasizes that there are BRD4-independent mechanisms that also promote AURKA expression, particularly in response to AURKA inhibition, and investigations into these mechanisms are warranted.

While I-BET151 and alisertib were significantly more efficacious together than alone, the combination had a delayed tumor regression effect. This led us to be concerned that there would also be impaired efficacy in any clinical translation. We hypothesized that a cytotoxic agent that could additionally induce tumor regression would augment the efficacy of dual BRD4 and AURKA inhibition to maintain durable disease control. As a proof of principle, we chose vincristine to test this hypothesis. Prior data showed that vincristine is synergistic with I-BET151 and alisertib individually [34,35]. Both studies showed that vincristine acted in combination with each drug to disrupt cell cycling, resulting in increased apoptosis. Vincristine is used sparingly in upfront neuroblastoma therapy due to limited single-agent efficacy, but it has improved efficacy in combination with drugs that cause cell cycle disruption [46–49], as also occurs with BRD4 and AUKRA inhibition. However, these drugs also have other impacts on neuroblastoma and cell biology, and additional studies are warranted to evaluate how vincristine-mediated effects interact with BRD4 and AURKA inhibition for antineoplastic effects. These include evaluations of microtubule dynamics and phosphorylation, cell cycle impairment, MYC/MYCN-dependent pathways such as phosphorylation of CDK7/9 [12], and activation of apoptotic and antiapoptotic pathways.

Clinically, vincristine is not significantly myelosuppressive, avoiding a toxicity associated with alisertib [17]. These features suggested that vincristine could be combined with BRD4 and AURKA inhibition in clinical trials for neuroblastoma. We did not anticipate increased toxicity with combined vincristine and I-BET151, requiring vincristine dose reduction, but we were encouraged to still see increased efficacy in the three-drug combination. Identification of other chemotherapeutic agents synergistic with BRD4 and AURKA inhibition, including other BRD4 inhibitors such as I-BET762 [50–52] and OTX015 [53,54], next-generation AURKA inhibitors [55], and/or other drugs in these classes, may find other combinations for clinical translation.

This study demonstrates that combined epigenetic and posttranslational targeting of oncogenic pathways can be synergistic. Whereas posttranslational targeting may cause rapid changes in oncogenic pathways, efficacy may be limited because of the transiency of effect. Epigenetic targeting of cancer cells may allow for more global and durable effects but can be limited by the slow cytotoxic effect, allowing tumors to grow before clinical efficacy can be appreciated. Dual epigenetic and posttranslational inhibition may improve clinical efficacy and also salvage drugs that have failed primary clinical endpoints when used alone. The drugs can be used together to increase antitumor efficacy, or they can also be dose-adjusted to

reduce toxicity while still maintaining or improving single-agent efficacy. The specific approach to target MYC/MYCN-driven oncogenic pathways may have broader impact on a host of cancer types in which these pathways are active, including medulloblastoma [56], rhabdomyosarcoma [57], pancreatic neuroendocrine tumors [58], prostatic neuroendocrine tumors [59], and breast cancer [60].

Conclusions

Our results demonstrate that combined epigenetic *MYC/MYCN* inhibition by use of the BRD4 inhibitor I-BET151 and posttranslational inhibition of MYC/MYCN stabilization by use of the Aurora Kinase A inhibitor alisertib are efficacious in antitumor effects against neuroblastoma with or without MYCN amplification. This combination approach is more effective in inducing and maintaining transcriptional and protein repression of multiple oncoproteins than each drug alone, and this is a likely driver of the drug combination's synergy. This antitumor effect is further improved with the addition of the antitubule chemotherapeutic vincristine, inducing durable tumor regressions in multiple tumor xenograft models of neuroblastoma *in vivo*. This study supports use of dual BRD4 and AURKA inhibition in clinical studies of neuroblastoma and other MYC/MYCN-driven malignancies.

Conflict of Interest

The authors declare on conflict of interest.

Appendix A. Supplementary data

Supplementary data to this article can be found online at https://doi.org/10.1016/j.neo.2018.08.002.

References

[1] Ladenstein R, et al (2017). Busulfan and melphalan versus carboplatin, etoposide, and melphalan as high-dose chemotherapy for high-risk neuroblastoma (HR-NBL1/SIOPEN): an international, randomised, multi-arm, open-label, phase 3 trial. *Lancet Oncol* **18**, 500–514. https://doi.org/:10.1016/S1470-2045(17)30070-0 [pmcid,].

[2] Erbe AK, et al (2017). Neuroblastoma Patients' KIR and KIR-ligand genotypes influence clinical outcome for dinutuximab-based immunotherapy: a report from the Children's Oncology Group. *Clin Cancer Res* . https://doi.org/:10.1158/1078-0432.CCR-17-1767 [pmcid,].

[3] London WB, et al (2017). Historical time to disease progression and progression-free survival in patients with recurrent/refractory neuroblastoma treated in the modern era on Children's Oncology Group early-phase trials. *Cancer* . https://doi.org/:10.1002/cncr.30934 [pmcid,].

[4] Brodeur GM, Seeger RC, Schwab M, Varmus HE, and Bishop JM (1984). Amplification of N-myc in untreated human neuroblastomas correlates with advanced disease stage. *Science* **224**, 1121–1124 [pmcid,].

[5] Wang LL, et al (2013). Neuroblastoma of undifferentiated subtype, prognostic significance of prominent nucleolar formation, and MYC/MYCN protein expression: a report from the Children's Oncology Group. *Cancer* **119**, 3718–3726. https://doi.org/:10.1002/cncr.28251 [pmcid: PMC4554323].

[6] Olsen RR, et al (2017). MYCN induces neuroblastoma in primary neural crest cells. *Oncogene* . https://doi.org/:10.1038/onc.2017.128 [pmcid,].

[7] Schwab M, et al (1984). Chromosome localization in normal human cells and neuroblastomas of a gene related to c-myc. *Nature* **308**, 288–291 [pmcid,].

[8] Jung M, et al (2017). A Myc activity signature predicts poor clinical outcomes in Myc-associated cancers. *Cancer Res* **77**, 971–981. https://doi.org/:10.1158/0008-5472.CAN-15-2906 [pmcid,].

[9] Fabian J, et al (2016). MYCN and HDAC5 transcriptionally repress CD9 to trigger invasion and metastasis in neuroblastoma. *Oncotarget* **7**, 66344–66359. https://doi.org/:10.18632/oncotarget.11662 [pmcid: PMC5341807].

[10] Duffy DJ, et al (2015). Integrative omics reveals MYCN as a global suppressor of cellular signalling and enables network-based therapeutic target discovery in neuroblastoma. *Oncotarget* **6**, 43182–43201. https://doi.org/:10.18632/oncotarget.6568 [pmcid: PMC4791225].

[11] Cowling VH and Cole MD (2007). The Myc transactivation domain promotes global phosphorylation of the RNA polymerase II carboxy-terminal domain independently of direct DNA binding. *Mol Cell Biol* **27**, 2059–2073. https://doi.org/:10.1128/MCB.01828-06 [pmcid: PMC1820498].

[12] Chipumuro E, et al (2014). CDK7 inhibition suppresses super-enhancer-linked oncogenic transcription in MYCN-driven cancer. *Cell* **159**, 1126–1139. https://doi.org/:10.1016/j.cell.2014.10.024 [pmcid: PMC4243043].

[13] Delehouze C, et al (2014). CDK/CK1 inhibitors roscovitine and CR8 downregulate amplified MYCN in neuroblastoma cells. *Oncogene* **33**, 5675–5687. https://doi.org/:10.1038/onc.2013.513 [pmcid: PMC4087096].

[14] Gopalan G, Chan CS, and Donovan PJ (1997). A novel mammalian, mitotic spindle-associated kinase is related to yeast and fly chromosome segregation regulators. *J Cell Biol* **138**, 643–656 [pmcid: PMC2141637].

[15] Otto T, et al (2009). Stabilization of N-Myc is a critical function of Aurora A in human neuroblastoma. *Cancer Cell* **15**, 67–78. https://doi.org/:10.1016/j.ccr.2008.12.005 [pmcid,].

[16] Carol H, et al (2011). Efficacy and pharmacokinetic/pharmacodynamic evaluation of the Aurora kinase A inhibitor MLN8237 against preclinical models of pediatric cancer. *Cancer Chemother Pharmacol* **68**, 1291–1304. https://doi.org/:10.1007/s00280-011-1618-8 [pmcid: 3215888].

[17] Mosse YP, et al (2012). Pediatric phase I trial and pharmacokinetic study of MLN8237, an investigational oral selective small-molecule inhibitor of Aurora kinase A: a Children's Oncology Group Phase I Consortium study. *Clin Cancer Res* **18**, 6058–6064. https://doi.org/:10.1158/1078-0432.CCR-11-3251 [pmcid: 4008248].

[18] Dickson MA, et al (2016). Phase II study of MLN8237 (Alisertib) in advanced/metastatic sarcoma. *Ann Oncol* **27**, 1855–1860. https://doi.org/:10.1093/annonc/mdw281 [pmcid: 5035789].

[19] Goldberg SL, et al (2014). An exploratory phase 2 study of investigational Aurora A kinase inhibitor alisertib (MLN8237) in acute myelogenous leukemia and myelodysplastic syndromes. *Leuk Res Rep* **3**, 58–61. https://doi.org/:10.1016/j.lrr.2014.06.003 [pmcid: PMC4110881].

[20] Matulonis UA, et al (2012). Phase II study of MLN8237 (alisertib), an investigational Aurora A kinase inhibitor, in patients with platinum-resistant or -refractory epithelial ovarian, fallopian tube, or primary peritoneal carcinoma. *Gynecol Oncol* **127**, 63–69. https://doi.org/:10.1016/j.ygyno.2012.06.040 [pmcid,].

[21] Hyman DM, et al (2017). A phase 2 study of alisertib (MLN8237) in recurrent or persistent uterine leiomyosarcoma: an NRG Oncology/Gynecologic Oncology Group study 0231D. *Gynecol Oncol* **144**, 96–100. https://doi.org/:10.1016/j.ygyno.2016.10.036 [pmcid: PMC5260802].

[22] Dey A, Chitsaz F, Abbasi A, Misteli T, and Ozato K (2003). The double bromodomain protein Brd4 binds to acetylated chromatin during interphase and mitosis. *Proc Natl Acad Sci U S A* **100**, 8758–8763. https://doi.org/:10.1073/pnas.1433065100 [pmcid: PMC166386].

[23] Jang MK, et al (2005). The bromodomain protein Brd4 is a positive regulatory component of P-TEFb and stimulates RNA polymerase II-dependent transcription. *Mol Cell* **19**, 523–534. https://doi.org/:10.1016/j.molcel.2005.06.027 [pmcid,].

[24] Sun B, et al (2015). Synergistic activity of BET protein antagonist-based combinations in mantle cell lymphoma cells sensitive or resistant to ibrutinib. *Blood* **126**, 1565–1574. https://doi.org/:10.1182/blood-2015-04-639542 [pmcid: PMC4582333].

[25] Wyce A, et al (2013). BET inhibition silences expression of MYCN and BCL2 and induces cytotoxicity in neuroblastoma tumor models. *PLoS One* **8**e72967. https://doi.org/:10.1371/journal.pone.0072967 [pmcid: PMC3751846].

[26] Bai L, et al (2017). Targeted degradation of BET proteins in triple-negative breast cancer. *Cancer Res* **77**, 2476–2487. https://doi.org/:10.1158/0008-5472.CAN-16-2622 [pmcid: PMC5413378].

[27] Zhao Y, et al (2016). High-resolution mapping of RNA polymerases identifies mechanisms of sensitivity and resistance to BET inhibitors in t(8;21) AML. *Cell Rep* **16**, 2003–2016. https://doi.org/:10.1016/j.celrep.2016.07.032 [pmcid: PMC4996374].

[28] Toyoshima M, et al (2012). Functional genomics identifies therapeutic targets for MYC-driven cancer. *Proc Natl Acad Sci U S A* **109**, 9545–9550. https://doi.org/:10.1073/pnas.1121119109 [pmcid: PMC3386069].

[29] Puissant A, et al (2013). Targeting MYCN in neuroblastoma by BET bromodomain inhibition. *Cancer Discov* **3**, 308–323. https://doi.org/: 10.1158/2159-8290.CD-12-0418 [pmcid: 3672953].

[30] Henssen A, et al (2016). Targeting MYCN-driven transcription by BET-bromodomain inhibition. *Clin Cancer Res* **22**, 2470–2481. https://doi.org/: 10.1158/1078-0432.CCR-15-1449 [pmcid,].

[31] Shah N, et al (2014). PBX1 is a favorable prognostic biomarker as it modulates 13-cis retinoic acid-mediated differentiation in neuroblastoma. *Clin Cancer Res* **20**, 4400–4412. https://doi.org/:10.1158/1078-0432.CCR-13-1486 [pmcid: 4134768].

[32] Maris JM, et al (2010). Initial testing of the aurora kinase A inhibitor MLN8237 by the Pediatric Preclinical Testing Program (PPTP). *Pediatr Blood Cancer* **55**, 26–34. https://doi.org/:10.1002/pbc.22430 [pmcid: PMC2874079].

[33] Chou TC and Talalay P (1984). Quantitative analysis of dose-effect relationships: the combined effects of multiple drugs or enzyme inhibitors. *Adv Enzym Regul* **22**, 27–55 [pmcid,].

[34] Liu PY, et al (2016). The BET bromodomain inhibitor exerts the most potent synergistic anticancer effects with quinone-containing compounds and anti--microtubule drugs. *Oncotarget* **7**, 79217–79232. https://doi.org/: 10.18632/oncotarget.12640 [pmcid: PMC5346709].

[35] Mahadevan D, et al (2012). Aurora A inhibitor (MLN8237) plus vincristine plus rituximab is synthetic lethal and a potential curative therapy in aggressive B-cell non-Hodgkin lymphoma. *Clin Cancer Res* **18**, 2210–2219. https://doi.org/: 10.1158/1078-0432.CCR-11-2413 [pmcid: PMC4607283].

[36] Matthay KK, et al (2016). Neuroblastoma. *Nat Rev Dis Primers* **2**, 16078. https://doi.org/:10.1038/nrdp.2016.78 [pmcid,].

[37] Zimmerman MW, et al (2017). c-MYC drives a subset of high-risk pediatric neuroblastomas and is activated through mechanisms including enhancer hijacking and focal enhancer amplification. *Cancer Discov* . https://doi.org/: 10.1158/2159-8290.CD-17-0993 [pmcid,].

[38] Wang LL, et al (2015). Augmented expression of MYC and/or MYCN protein defines highly aggressive MYC-driven neuroblastoma: a Children's Oncology Group study. *Br J Cancer* **113**, 57–63. https://doi.org/:10.1038/bjc.2015.188 [pmcid: PMC4647535].

[39] Brockmann M, et al (2016). Small molecule inhibitors of Aurora-A induce proteasomal degradation of N-Myc in childhood neuroblastoma. *Cancer Cell* **30**, 357–358. https://doi.org/:10.1016/j.ccell.2016.07.002 [pmcid,].

[40] Attiyeh EF, et al (2005). Chromosome 1p and 11q deletions and outcome in neuroblastoma. *N Engl J Med* **353**, 2243–2253. https://doi.org/:10.1056/NEJ-Moa052399 [pmcid,].

[41] Cohn SL, et al (2009). The International Neuroblastoma Risk Group (INRG) classification system: an INRG Task Force report. *J Clin Oncol* **27**, 289–297. https://doi.org/:10.1200/JCO.2008.16.6785 [pmcid: PMC2650388].

[42] Lestini BJ, et al (2009). Mcl1 downregulation sensitizes neuroblastoma to cytotoxic chemotherapy and small molecule Bcl2-family antagonists. *Cancer Biol Ther* **8**, 1587–1595 [pmcid: 3770183].

[43] Dijkhuis AJ, Klappe K, Kamps W, Sietsma H, and Kok JW (2006). Gangliosides do not affect ABC transporter function in human neuroblastoma cells. *J Lipid Res* **47**, 1187–1195. https://doi.org/:10.1194/jlr.M500518-JLR200 [pmcid,].

[44] Dijkhuis AJ, Douwes J, Kamps W, Sietsma H, and Kok JW (2003). Differential expression of sphingolipids in P-glycoprotein or multidrug resistance-related protein 1 expressing human neuroblastoma cell lines. *FEBS Lett* **548**, 28–32 [pmcid,].

[45] First multicenter, randomized phase 3 study in patients (Pts) with relapsed/refractory (R/R) peripheral T-cell lymphoma (PTCL): alisertib (MLN8237) versus investigator's choice (LUMIERE trial; NCT01482962). *Clin Adv Hematol Oncol* **14**, 12–13 [pmcid,].

[46] Kollareddy M, et al (2017). The small molecule inhibitor YK-4-279 disrupts mitotic progression of neuroblastoma cells, overcomes drug resistance and synergizes with inhibitors of mitosis. *Cancer Lett* **403**, 74–85. https://doi.org/: 10.1016/j.canlet.2017.05.027 [pmcid: PMC5542135].

[47] Langemann D, et al (2017). Sensitization of neuroblastoma for vincristine-induced apoptosis by Smac mimetic LCL161 is attended by G2 cell cycle arrest but is independent of NFkappaB, RIP1 and TNF-alpha. *Oncotarget* **8**, 87763–87772. https://doi.org/:10.18632/oncotarget.21193 [pmcid: PMC5675670].

[48] Amoroso L, et al (2018). Topotecan-vincristine-doxorubicin in stage 4 high-risk neuroblastoma patients failing to achieve a complete metastatic response to rapid COJEC: A SIOPEN study. *Cancer Res Treat* **50**, 148–155. https://doi.org/: 10.4143/crt.2016.511 [pmcid: PMC5784636].

[49] Zollner SK, et al (2017). Inhibition of the oncogenic fusion protein EWS-FLI1 causes G2-M cell cycle arrest and enhanced vincristine sensitivity in Ewing's sarcoma. *Sci Signal* **10**. https://doi.org/:10.1126/scisignal.aam8429 [pmcid,].

[50] Leal AS, et al (2017). Bromodomain inhibitors, JQ1 and I-BET 762, as potential therapies for pancreatic cancer. *Cancer Lett* **394**, 76–87. https://doi.org/: 10.1016/j.canlet.2017.02.021 [pmcid,].

[51] Chaidos A, et al (2014). Potent antimyeloma activity of the novel bromodomain inhibitors I-BET151 and I-BET762. *Blood* **123**, 697–705. https://doi.org/: 10.1182/blood-2013-01-478420 [pmcid,].

[52] Zhao Y, Yang CY, and Wang S (2013). The making of I-BET762, a BET bromodomain inhibitor now in clinical development. *J Med Chem* **56**, 7498–7500. https://doi.org/:10.1021/jm4014407 [pmcid,].

[53] Stathis A, et al (2016). Clinical response of carcinomas harboring the BRD4-NUT oncoprotein to the targeted bromodomain inhibitor OTX015/MK-8628. *Cancer Discov* **6**, 492–500. https://doi.org/: 10.1158/2159-8290.CD-15-1335 [pmcid: PMC4854801].

[54] Boi M, et al (2015). The BET bromodomain inhibitor OTX015 affects pathogenetic pathways in preclinical B-cell tumor models and synergizes with targeted drugs. *Clin Cancer Res* **21**, 1628–1638. https://doi.org/: 10.1158/1078-0432.CCR-14-1561 [pmcid,].

[55] Gustafson WC, et al (2014). Drugging MYCN through an allosteric transition in Aurora kinase A. *Cancer Cell* **26**, 414–427. https://doi.org/: 10.1016/j.ccr.2014.07.015 [pmcid: 4160413].

[56] Cavalli FMG, et al (2017). Intertumoral heterogeneity within medulloblastoma subgroups. *Cancer Cell* **31**, 737–754.e736. https://doi.org/: 10.1016/j.ccell.2017.05.005 [pmcid,].

[57] Tonelli R, et al (2012). Antitumor activity of sustained N-myc reduction in rhabdomyosarcomas and transcriptional block by antigene therapy. *Clin Cancer Res* **18**, 796–807. https://doi.org/:10.1158/1078-0432.CCR-11-1981 [pmcid,].

[58] Mosquera JM, et al (2013). Concurrent AURKA and MYCN gene amplifications are harbingers of lethal treatment-related neuroendocrine prostate cancer. *Neoplasia* **15**, 1–10 [pmcid: PMC3556934].

[59] Zhang W, et al (2018). Targeting the MYCN-PARP-DNA Damage Response Pathway in Neuroendocrine Prostate Cancer. *Clin Cancer Res* **24**, 696–707. https://doi.org/:10.1158/1078-0432.CCR-17-1872 [pmcid: PMC5823274].

[60] Deming SL, Nass SJ, Dickson RB, and Trock BJ (2000). C-myc amplification in breast cancer: a meta-analysis of its occurrence and prognostic relevance. *Br J Cancer* **83**, 1688–1695. https://doi.org/:10.1054/bjoc.2000.1522 [pmcid: PMC2363455].